

# A Case Study of Flood Modeling with Adaptive Mesh Refinement

WENTAO GONG

*Graduate school of engineering, Hokkaido University, Sapporo, Japan, wentaogong@yahoo.com*

YASUYUKI SHIMIZU

*Faculty of engineering, Hokkaido University, Sapporo, Japan, yasu@eng.hokudai.ac.jp*

TOSHIKI IWASAKI

*Faculty of engineering, Hokkaido University, Sapporo, Japan, tiwasaki@eng.hokudai.ac.jp*

## ABSTRACT

In this study, we propose an urban flood modeling framework using Adaptive Mesh Refinement (AMR) technique, which has been developed as an effective way of reducing the computational cost but guaranteeing the computational accuracy. AMR is able to refine or de-refine the computational grid resolution in space and time when necessary. We implement the AMR method to a two-dimensional shallow water flow model, which is solved by using the separation method and constrained interpolation profile (CIP) technique, for flood simulation. The proposed model is then applied to a case of urban flood in Sapporo, Japan. We investigate various refinement criteria to investigate the performance of flood modeling with AMR (i.e., accuracy and efficiency). The fixed fine grid model and fixed coarse grid model are also tested as a comparison with the AMR. The results show that the AMR saves the 47%-68.2% computational time with a reasonable accuracy of flood characteristics.

*Keywords:* Adaptive mesh refinement (AMR), CIP, Flood modeling, Shallow water flow model, Computational time

## 1. INTRODUCTION

It may be a general understanding that climate change has caused a lot of natural disasters such as heavy rainfall, flood, and debris flow in the last few years, resulting in a great loss of people's lives and property. Several computational technologies have been nowadays an important tool for mitigating the damage due to the natural disasters by predicting risk and hazard in advance. In this study, we focus on the flooding in extensively developed and populated urban areas. In the last decades, urban floods have become a growing concern as a consequence of concentration of population and economic factors. It means that an urban flood modeling can provide the detailed information in terms of flood characteristics, contributing decision making of some countermeasures for flooding and evacuation plans for residential people. However, a flood modeling in a large scale domain with complicated bed geometry and infrastructure arrangement will be a difficult task due to the expensive computation cost.

To solve this problem, many techniques have been developed in the past a decade. These approaches include: reduced-complexity models (Liu and Pender, 2010), parallelization (Hankin et al., 2008; Neal et al., 2010), unstructured mesh (Wang et al., 2010), adaptive grid-based methods (Wang and Liang, 2011), grid coarsening (Yu and Lane, 2006a), and hyper grid method (Morikawa and Kimura, 2018). Among these methods, the grid coarsening and hyper grid method are straightforward to reduce the computation time. However, the low resolution leads to the loss of information and less accuracy of modeling results.

Adaptive mesh refinement (AMR) proposed by Berger et al. (1984) is one of the computational techniques contributing both reducing the computational cost and guaranteeing the accuracy. This method can recursively refine the parts of domain, where the model requires the high resolution. So far, lots of researchers have developed the flood modeling with AMR (e.g., Wang and Liang, 2011; Chen et al. 2012; Huang et al. 2015). Wang and Liang, (2011) simulated a laboratory-scale dam break flow over a triangular obstacle and slow varying flood inundation at the Thamesmead with the AMR which saved the 3.5 times on the run time compared with the uniform, high resolution computational grid. However, they just use the first order finite volume, Godunov-type scheme to solve the shallow water flow model. Chen et al. (2012) performed a 2D urban flood modeling with AMR. They used the 2D non-inertia urban inundation model, based on the shallow flow modeling for overland flow propagation with mild natural topography and implemented the building coverage ratio and conveyance reduction factors coefficients. Huang et al. (2015) described a couple 2D shallow watery hydrodynamic and non-capacity sediment transport model with AMR and saved the 80% to 93% CPU time.

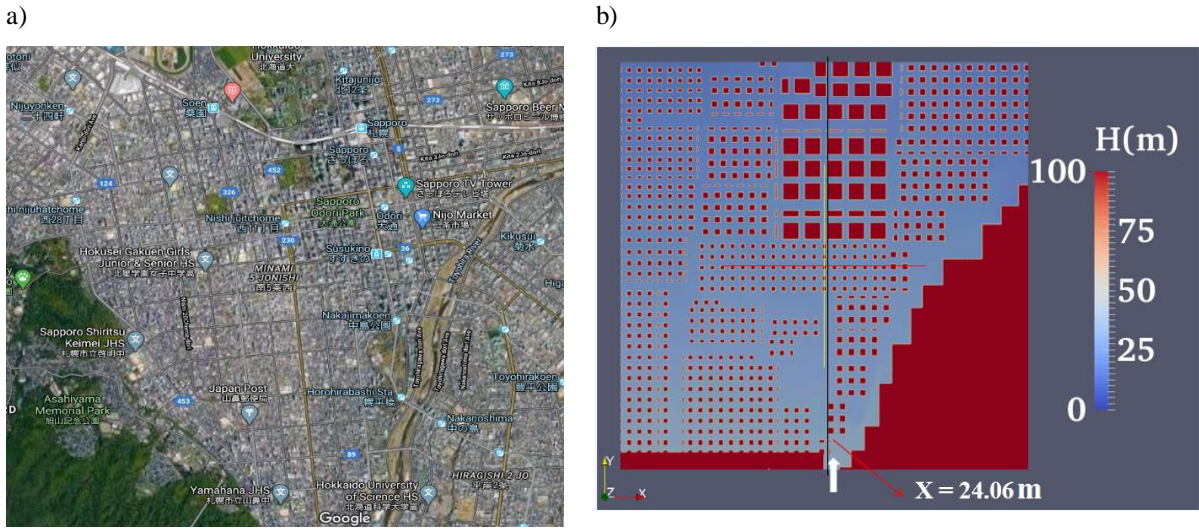


Figure 1. a) The center of Sapporo city, Japan. b) Modelled elevation data of the objective area (Morikawa (2019)).

In this paper, we propose an urban flood modeling framework by using a high-accuracy shallow water flow model and the AMR technique. The shallow water flow model is solved by using separation technique and the CIP method for advection term to minimize the numerical diffusion. We then implement the AMR method into the proposed shallow flow modeling. The model is applied to a case of urban flooding in Sapporo city, Japan. For this simulation, we use a terrain elevation data that includes the building height and the position, which is complicated enough to check robustness of the proposed model. We also investigate the various refinement criteria to observe the performance of flood modeling with AMR.

## 2. COMPUTATIONAL MODEL

### 2.1 Shallow water flow model with Adaptive mesh refinement

We implement a block-based AMR method proposed by MacNeice et al. (2000), which have been distributed as a package, PARAMESH, into a two-dimensional flood modeling. The grid resolution can be spatially or temporally refined or de-refined by using this technique based on refinement criteria (which will be explained in section 2.2). By using this method, we can obtain high (low) resolution computational grid when necessary (or not), saving the computational cost dynamically. This method builds a hierarchy of sub-grids to cover the domain and all the blocks have identical logical structure. In this study, we set  $10 \times 10$  grid in each block. When the model suggest refining a block (parent block) based on the criteria we set, the first step would produce 4 child blocks, and each with its own  $10 \times 10$  meshes, but now with the mesh spacing one-half that of parent block. Any or all of these children can themselves be refined in the same manner. The process continues, until the refinement level up to maximum where the spatial resolution will become high. Based on the same rules, when the model suggests de-refinement, a coarse step will happen until the refinement level decrease to minimum where the resolution is low.

A two-dimensional shallow water flow model is used for flood simulation. In this model, Manning's roughness model is utilized for evaluating the bed shear stress. We basically use a computational method proposed by Jang and Shimizu (2005) to solve the governing equation numerically. The governing equations of the model are discretized on a staggered grid coordinate system as shown in Fig. 2, namely, the scalar value like water depth,  $h$ , is defined at the center of cell, and vector value like flow velocities in each direction,  $u$ ,  $v$ , are defined at the boundary of cell. The momentum equation is decomposed into advection phase and non-advection phase. We implicitly predict a first-step flow field by iterating momentum equation of non-advection phase and continuity equation of water and then the constrained interpolation profile (CIP) method is used to solve the advection phase for calculating the flow velocity at next time step. The flux conservation is also considered, because the fluxes on a common block boundary between two blocks at different refinement level are not likely to be consistent and the fluxes on the more refined block are more accurate. So, the fluxes entering or leaving a grid cell through a common cell face shared with 4 cells of a more refined neighbor, should equal the sum of the fluxes across the appropriate faces of the 4 smaller cells.

### 2.2 Computational condition

The proposed flood model with AMR is applied to a case of flooding in Sapporo, Japan. The objective area of this study is shown in Fig.1a. Fig.1a shows that the objective area is highly urbanized by a lot of buildings. To consider this complicated arrangement of the buildings on the flood calculation, we use a same way used by Morikawa (2019), who modeled a small-scale experiment regarding the urban flood in Sapporo used in Miura

Table 1. The calculation condition of the computational model.

<b>Computational domain</b>		2800 m x 2800 m
<b>Manning's roughness coefs.</b>		0.03
<b>Water discharge</b>		771 m <sup>3</sup> /s
<b>AMR</b>	<b>minimum refinement level (level 1)</b>	280 m x 280 m
	<b>Maximum refinement level (level 7)</b>	4.4 m x 4.4 m
<b>Fine grid model</b>		4.4 m x 4.4 m
<b>Coarse grid model</b>		17.5m x 17.5m
<b>Calculation end time</b>		2000 seconds

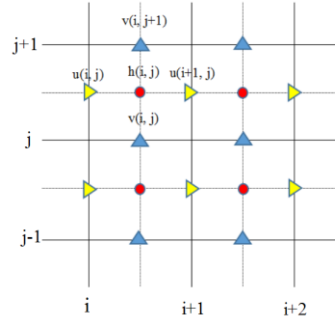


Figure 2. The location of the  $h$  (water depth),  $u$ ,  $v$  (flow velocities in  $x$  and  $y$  directions) on the staggered grid

et al. (2011) to a real-scale flood simulation. The elevation data set of which the special resolution is 10m in each direction is developed based on the laser profile elevation measurement, and the building is considered as a high elevation area on the elevation data as shown in Fig. 1b.

In this elevation data, the different spatial density of building is also modelled based on the aerial photograph (i.e., Fig. 1a). When refinement or de-refinement is taken place in the computation, this elevation data is interpolated into every node of the computational grid by weighted averaging as,

$$\eta = \frac{\sum z / r}{\sum 1 / r} \quad (1)$$

where  $z$  represents the elevation data,  $\eta$  is the elevation at the computational node, and  $r$  is the distance between the elevation data and grid node. The window size for searching the elevation data for this averaging is set to be local grid size. If there is no data within this window size, the elevation of nearest data is used for the elevation of the computational node.

We impose a constant water discharge from the bottom edge of the computational domain in Fig. 1b, which is denoted by an arrow in the figure. Other three boundaries are treated as a no-flux boundary (i.e., like wall) for simplicity. In addition, the Manning's roughness coefficient is set to be 0.03 in entire computational domain.

Table 1 shows the basic information in this computational model. For the cases of AMR calculation, we set the minimum and maximum refinement level of the AMR as 1 and 7. It means that the grid sizes of minimum and maximum refinement levels are 280 m and 4.4 m, respectively, since we set 10 x 10 grids for each block. To check the accuracy and efficiency of AMR method, the fine and coarse fixed grid models are also used. The grid size of fine grid model is 4.4 m (the refinement level is fixed as Level 7), and the grid size of coarse grid model is 17.5 m (the refinement level is fixed as Level 5).

The different refinement criteria are tested on this flood modeling, which includes  $\frac{\Delta h}{h}$ ,  $\frac{\Delta v}{v}$ ,  $\frac{\Delta h}{\Delta x}$ ,  $\frac{\Delta h}{\Delta y}$ ,  $\Delta v$ ,  $\Delta h$  In Figure 2, the cell centered data  $h(i, j)$  is physically located between boundary centered data  $u(i, j)$  and  $u(i+1, j)$ , between  $v(i, j)$  and  $v(i, j+1)$ . The  $h$  means the water depth and  $u$ ,  $v$  mean the velocity in  $x$  direction and  $y$  direction respectively.  $\Delta h$  and  $\Delta v$  mean the absolute value of water depth and flow velocity magnitude difference between two grid point for every four directions, respectively. The  $\Delta x$  and  $\Delta y$  are the grid size in  $x$  and  $y$  directions, respectively. Every time step, the values of these refinement criteria will be calculated, then the maximum values of these refinement criteria in each block are used to determine refinement/de-refinement by the upper value and lower value of the threshold value showed in Table 2. We test these criteria above to obtain the maximum number of the meshes and computational time, then based on that, the efficiency of these refinement criteria are evaluated. Meanwhile, the accuracy and the phenomenon of each case are checked too.

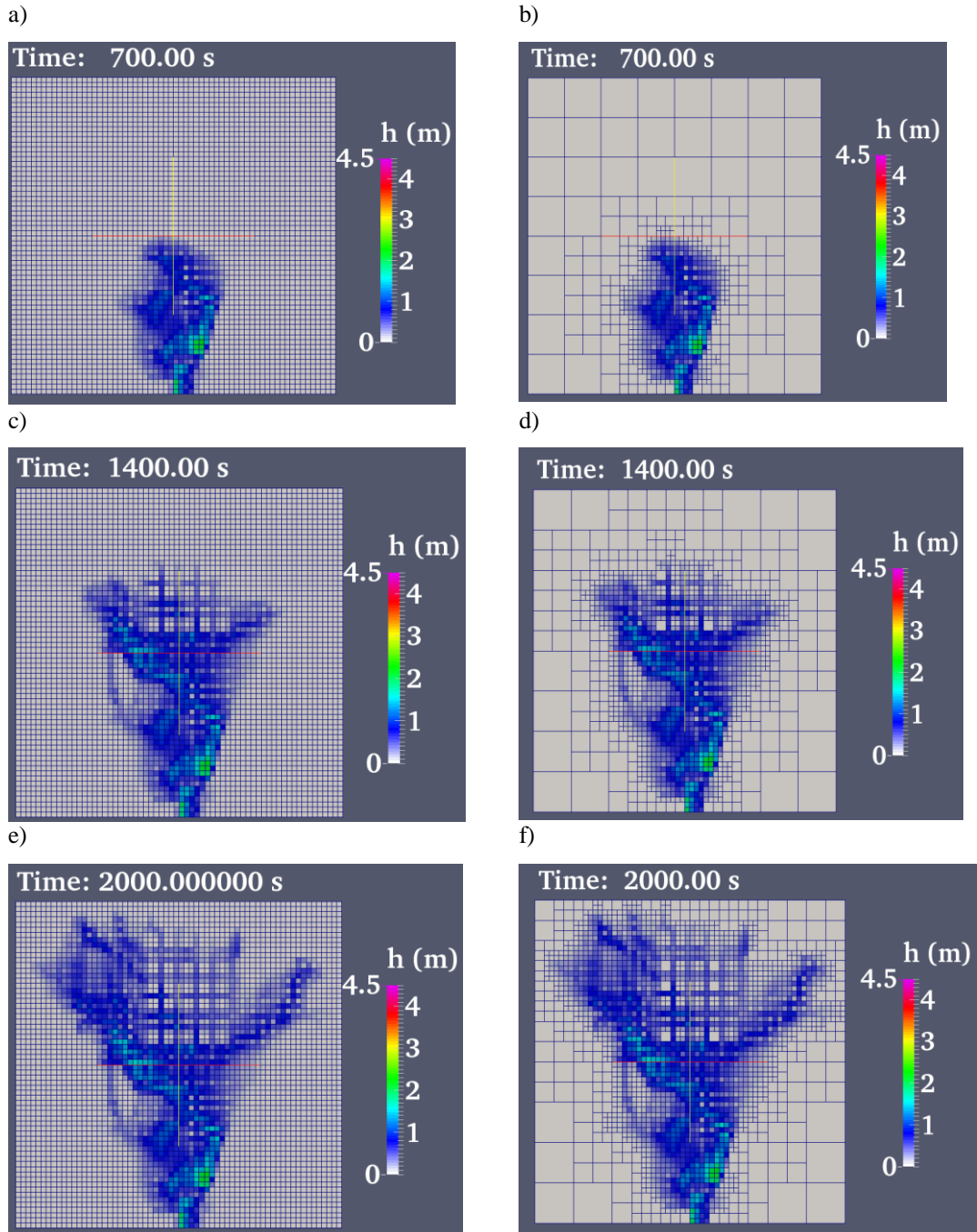


Figure 3. The temporal change of water depth. a), c) and e) fine-grid case and the b), d) and f) AMR case at 700, 1400 and 2000 seconds, respectively.

### 3. RESULTS AND DISCUSSION

#### 3.1 The accuracy of the flood simulation

Firstly, we compare the water depth (Fig.3) and flow velocity (Fig.4) of the flood modeling between the AMR case and the fixed fine grid case. For the AMR calculation, the relative velocity difference (i.e.,  $\Delta v/v$ ) is used for the refinement criteria (see AMR1 on Table 2).

Figures 3b, d, and f show that the computational grid is spatially refined depending on the flood propagation but the grid remains coarse where there is no flood flow. The comparison of the water depth also shows that the AMR case reasonably captures the temporal change of water depth (i.e., flood propagation) simulated by the fine-grid model (Figs 3a, c, and e). In addition, as shown in Figure 4, the flow velocity simulated in the fine-grid model and AMR are almost identical.

Figure 5 visualizes the one-dimensional view of water depths of the grid point along a downstream direction as indicated in the black line in Fig. 1b at 2000 seconds. In addition, Figure 6 shows the temporal change of the location of flooding (i.e., the location of the head of the flood flow along the black line shown in Fig. 1b), describing how fast the flood propagates in downstream direction. Both figures indicate that the AMR correctly simulate the result of fine grid case, capturing inundation depth and flood propagation speed. The coarse grid

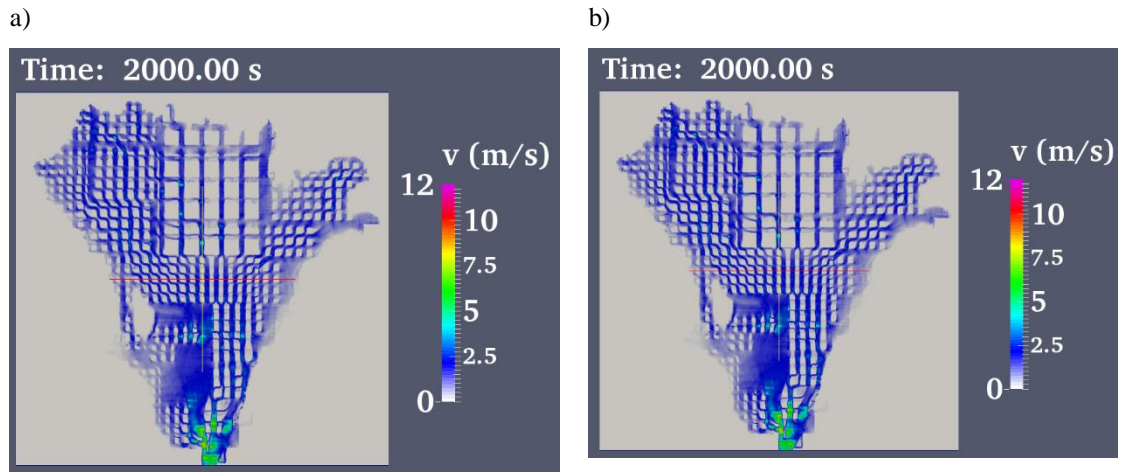


Figure 4. The velocity distribution of a) fine grid case, b) AMR case at 2000 seconds.

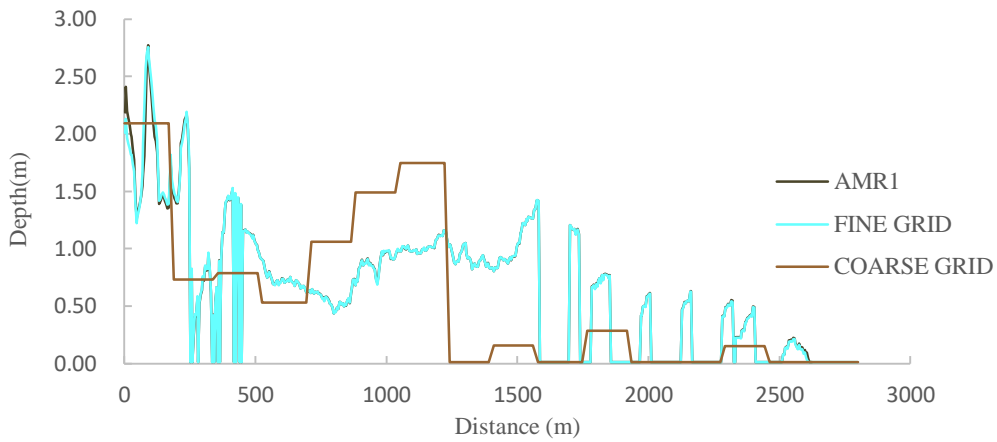


Figure 5. The water depth along the black line defined in Fig. 1b on the AMR case, fine grid and the coarse grid model, respectively.

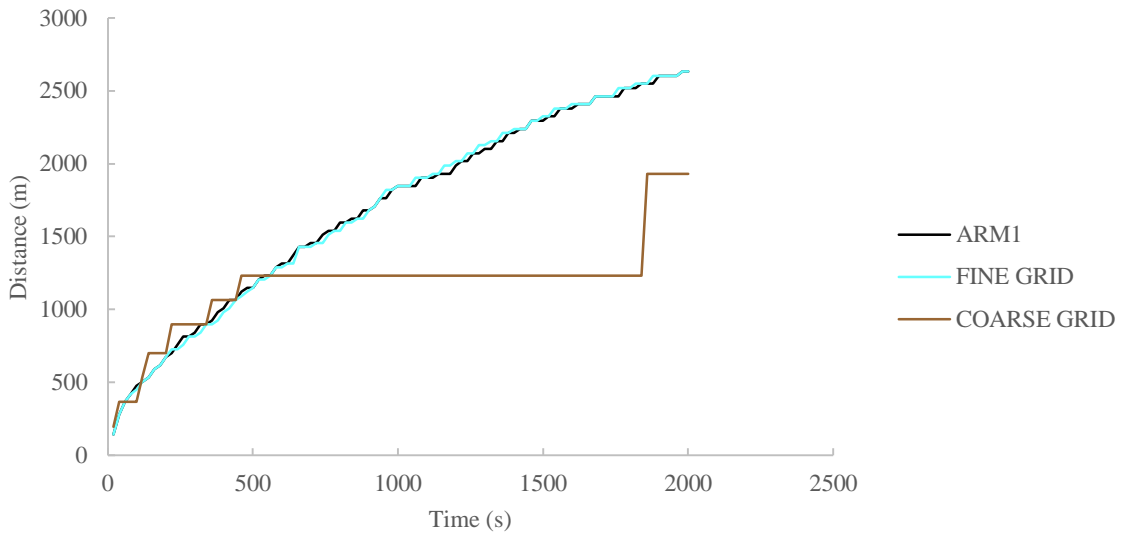


Figure 6. Temporal change of the location of the front inundated area from the upstream inflow along the black line defined in Fig. 1b.

model partly captures these flow feature in the upstream area, where the spatial density of buildings is not very high, but completely fails to reproduce these features in downstream area, where the building density is high. This is obviously because that the coarse model cannot represent complicated bed geometry, which is mostly caused by a lot of buildings.



Table 2. The results of the AMR with different refinement criteria and the fixed fine grid.

Refinement Criteria		Threshold value		Refinement level		Number of meshes	Computational Time
		upper value (refine)	lower value (derefine)	Min.	Max.		
AMR1	$\frac{\Delta v}{v}$	0.35	0.25	4	7	314900	3h37min
AMR2	$\frac{\Delta h}{h}$	0.24	0.09	1	6	74100	39min
AMR3	$\frac{\Delta h}{h}$	0.35	0.25	1	7	384900	5h42min
AMR4	$\frac{\Delta h}{h}$	0.24	0.09	1	7	380500	3h39min
AMR5	$\frac{\Delta h}{\Delta x}, \frac{\Delta h}{\Delta y}$	0.005	0.0005	1	7	306900	3h25min
AMR6	$\Delta h$	0.05	0.002	3	7	306900	3h36min
AMR7	$\Delta v$	0.05	0.002	1	7	314900	3h37min
-	Fine grid	-	-	-	-	546100	10h45min

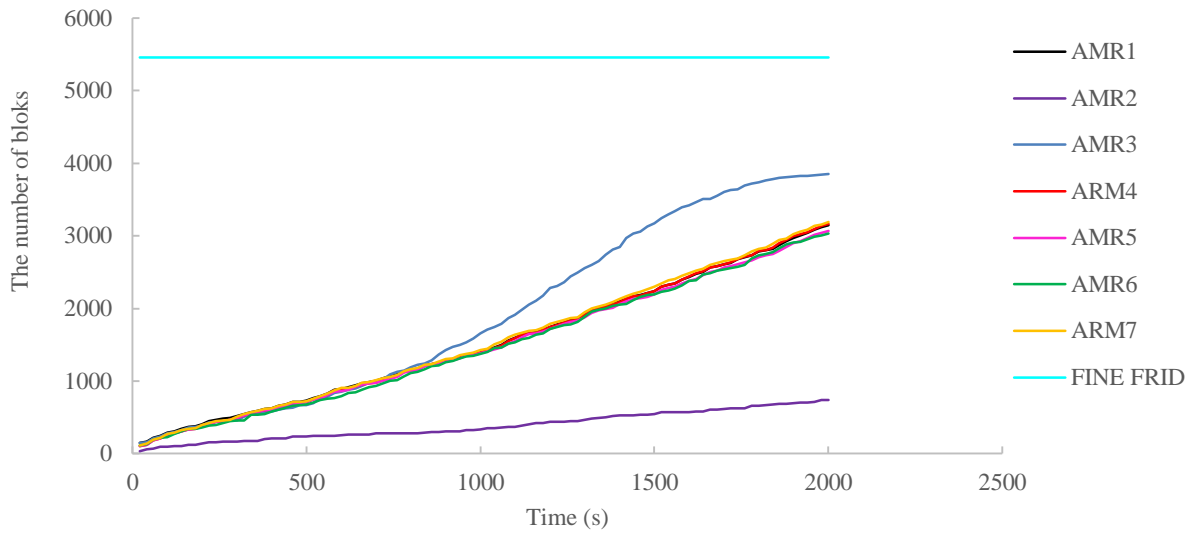


Figure 7. The distances from the upstream inflow at different time.

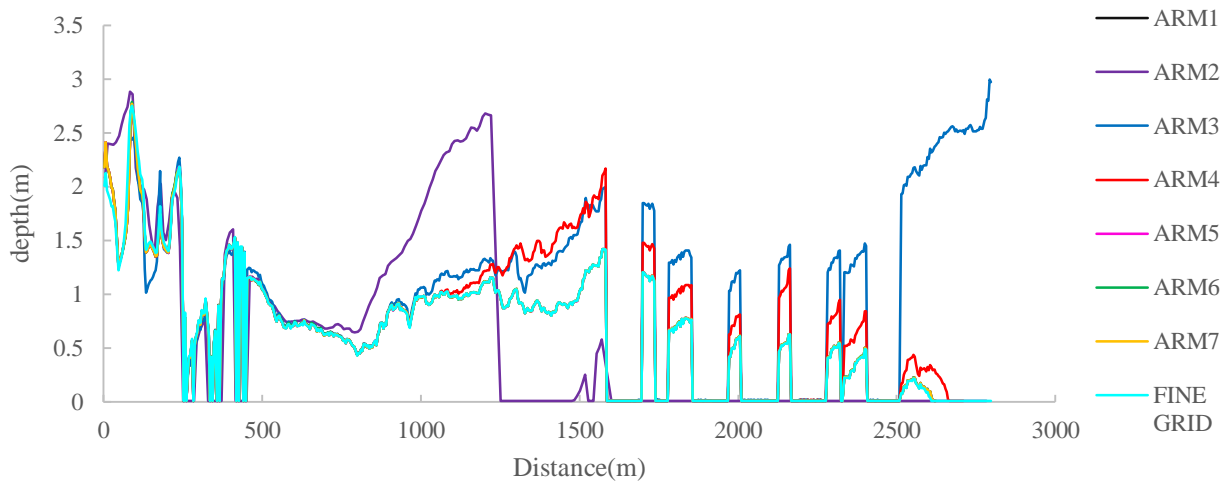


Figure 8. The water depths along the black line (showed in Fig. 1b) at 2000s on various refinement criteria and the fine grid case.

This result suggests that the proposed flood model with AMR is able to capture result obtained by the high-resolution, but uniform fine grid without significant loss of the accuracy but greatly reducing the computational grid number.

### 3.2 The evaluation of the refinement criteria and the efficiency of the flood simulation

Table 2 shows several refinement criteria we tested (defined as AMR1 to AMR7) and resulted computational time for flood simulation. In addition, Figure 7 shows the temporal change of the number of the blocks on the various refinement criteria and the fine grid case, and Figure 8 shows simulated water depth in the downstream direction along the black line in the Fig. 1a. We firstly show the effect of threshold value and refinement level for the refinement

in same criteria in the runs of AMR2, 3, 4. Among these runs, AMR4 is the only case reproducing the result obtained by the fine grid model due to the appropriate threshold value and refinement level, respectively. AMR2 gives the shortest computational time among all computational run, however, the computational result is not acceptable as shown in Fig. 8. This is because that the maximum refinement level which is equal to 6 is insufficient to resolve the highly urbanized area in the computational domain. The AMR3 generates much computational blocks, so that it needed the computational time (efficiency compared with fine grid case is just 47%). In this ARM3, the lower value set for de-refinement is close to the upper value set for refinement (the lower value is too large), which leads to the grid coarsening and inaccurate water depth on the high density building area compared with the fine grid model. This result suggests that suitable values has to be calibrated for the refinement level and threshold value.

Table 2, Figs. 7 and 8 also show that AMR 1, 5, 6 and 7 obtained the similar computational time and accuracy, which results are also same with the fine grid model as shown in Fig. 8. Among them, AMR5 is the most efficient, which saves 68.2% time. The physical meaning of this criteria is water surface slope, so that it may be relatively easy to calibrate the parameter in the physical sense rather than other parameters we tested.

## 4. CONCLUSIONS

In this study, we simulate a flooding in an urban area by using a two dimensional shallow flow model with Adaptive mesh refinement. We tested several criteria, which determine how we refine the computational grid in space and time, to check the computational efficiency and accuracy. The results showed that AMR can save 47%-68.2% computational time without significant loss of computational accuracy. However, the accuracy and efficiency differ, depending on the refinement criteria and the threshold values. For the high density building area, the high resolution is needed; otherwise we cannot capture detail flow characteristics. The results also suggest however that the criteria and threshold value for refinement need to be calibrated carefully to obtain the reasonable result. The refinement criteria tested here can be improved further in order to find the optimal solution by using more effective mathematical techniques.

## REFERENCES

- Ali, M. A., Kimura, I. and Shimizu, Y. (2016). Flood modelling using sub - grid based finite volume approach & constrained interpolation profile method. *In Proceedings of the International Conference on Fluvial Hydraulics (River Flow 2016)*. Iowa City, USA: CRC Press, 1891-1895.
- Bates, P. D., Horritt, M. S., and Fewtrell, T. J. (2010). A simple inertial formulation of the shallow water equations for efficient two-dimensional flood inundation modelling. *Journal of Hydrology*, 387(1-2), 33-45.
- Berger, M.J., Colella, P. (1989). Local adaptive mesh refinement for shock hydrodynamics. *J. Comput. Phys.* 82, 64-84. doi:10.1016/0021-9991(89)90035-1
- Berger, M.J., Oliger, J. (1984). Adaptive mesh refinement for hyperbolic partial differential equations. *J. Comput. Phys.* 53(3), 484-512. doi:10.1016/0021-9991(84)90073-1415- 427.
- Chen, A. S., Evans, B., Djordjević, S., and Savić, D. A. (2012). Multi-layered coarse grid modelling in 2D urban flood simulations. *Journal of Hydrology*, 470, 1-11.
- Cobby, D. M., Mason, D. C., and Davenport, I. J. (2001). Image processing of airborne scanning laser altimetry data for improved river flood modelling. *ISPRS Journal of Photogrammetry and Remote Sensing*, 56(2), 121-138.
- Hankin, B., Waller, S., Astle, G., and Kellagher, R. (2008). Mapping space for water: screening for urban flash flooding. *Journal of Flood Risk Management*, 1(1), 13-22.
- Huang, W., Cao, Z., Pender, G., Liu, Q., and Carling, P. (2015). Coupled flood and sediment transport modelling with adaptive mesh refinement. *Science China Technological Sciences*, 58(8), 1425-1438.
- Jang, C.L. and Shimizu, Y. (2005). Numerical simulation of relatively wide, shallow channels with erodible banks. *Journal of Hydraulic Engineering*, 131(7), 565-575.
- Liu, Y., and Pender, G. (2010). A new rapid flood inundation model. *In proceedings of the first IAHR European Congress*, 4-6.

- Morikawa, G. (2019). Numerical analysis of flood with hyper grid model, dissertation for Master degree of Hokkaido University, Sapporo, Japan.
- Morikawa, G. and Kimura, I. (2018). Numerical analysis of flood with a double grid model. *In E3S Web of Conferences* (Vol. 40, p. 05042). EDP Sciences.
- MacNeice, P., Olson, K.M., Mobarry, C., Fainchtein, R. and Packer, C. (2000). PARAMESH: A parallel Adaptive Mesh Refinement Community Toolkit. *Computer Physics Communications*, 126(3), 330-354.
- Miura, S., Kawamura, I., Kimura, I., and Miura, A. (2011). Study on inundation flow analysis method in densely populated urban area on alluvial fan. *Journal of Japan Society of Civil Engineers, Ser. B1 (Hydraulic Engineering)*, 67, I\_979-I\_984.
- Neal, J. C., Fewtrell, T. J., Bates, P. D., and Wright, N. G. (2010). A comparison of three parallelization methods for 2D flood inundation models. *Environmental Modelling & Software*, 25(4), 398-411.
- Wang, J. P., and Liang, Q. (2011). Testing a new adaptive grid based shallow flow model for different types of flood simulations. *Journal of Flood Risk Management*, 4(2), 96-103.